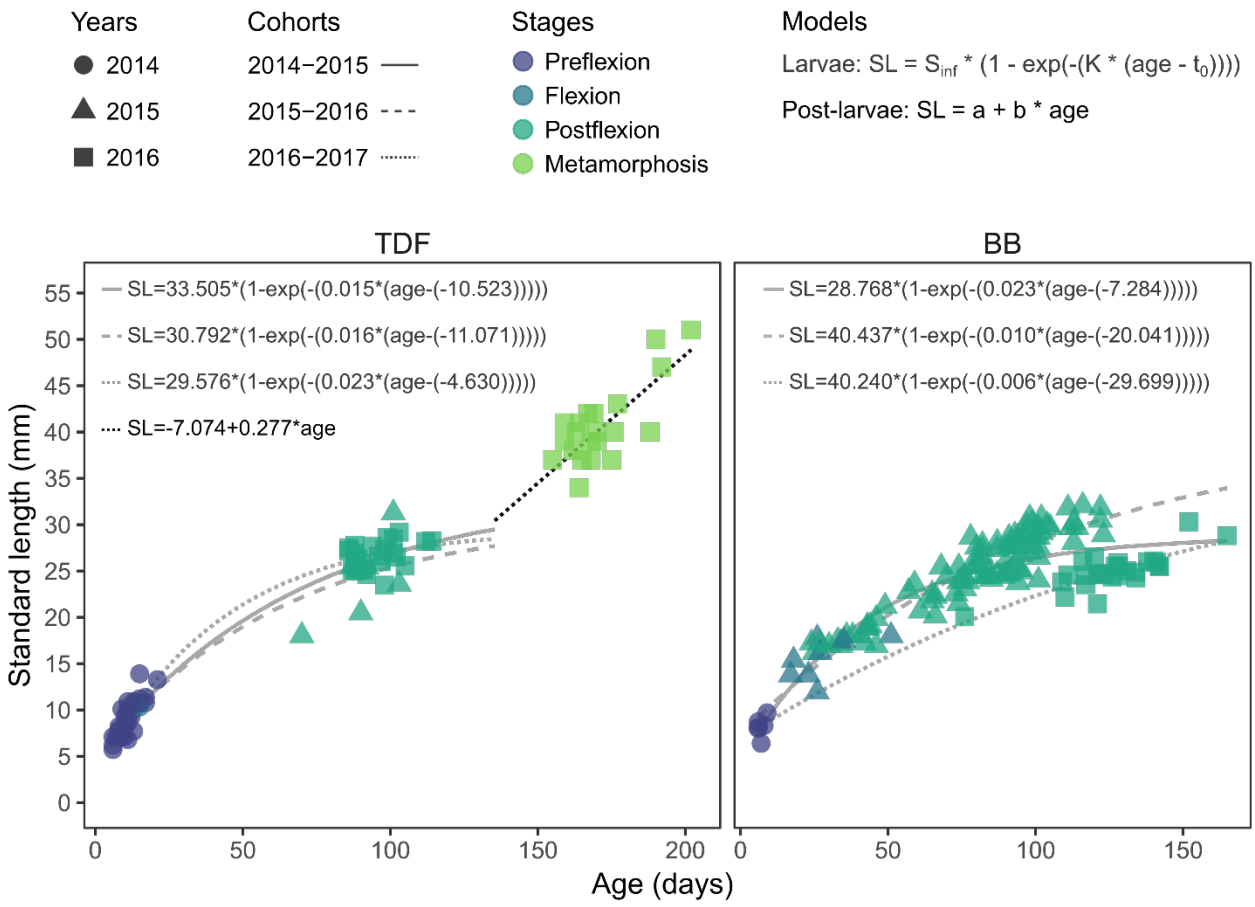

Fig. S1. Description of the data and models employed to estimate Fuegian sprat ages and spawning dates. Otolith microstructure analyses were performed on sprat captured in the surveys of spring of 2014 and autumns of 2016 and 2017. Estimated individual ages and measured standard lengths (SL) were employed to fit models for each area (TDF and BB) and cohort independently: 2014-2015 (solid lines), 2015-2016 (dashed lines) and 2016-2017 (dotted lines). A Von Bertalanffy model was used for larval specimens (parameters: S_{inf}, K and t_0) employing data from preflexion larvae captured in 2014 as the initial condition of all curves and data from older larvae (flexion and postflexion) captured in autumn as the final condition for each cohort. Due to the lack of older larvae for the 2014-2015 cohort, the model was fitted to data from both autumns (2016 and 2017). A linear model was selected for post-larval specimens (parameters: a and b). Sprat ages were back calculated as a function of SL and spawning dates were estimated as ages minus 5 or 7 days for TDF and the BB respectively as seen for *S. sprattus* reared at equivalent mean temperatures to those measured in situ in both habitats (8°C and 6°C) (Milligan 1986).

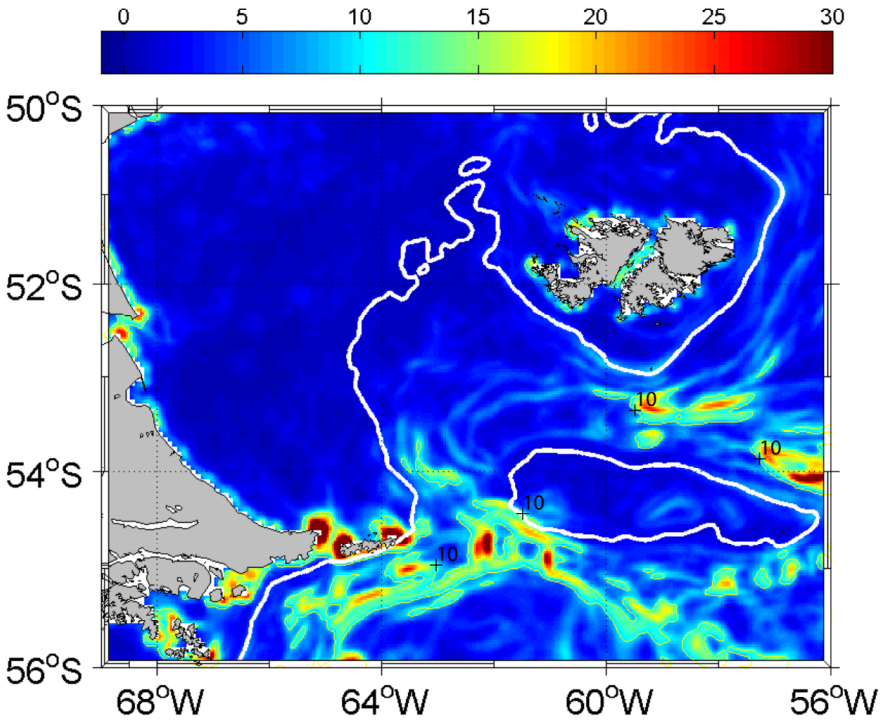

Fig. S2. Mean annual horizontal diffusivity (K_h; m s^{-2}) in the study area estimated using the Smagorinsky equation (Smagorinsky 1963).

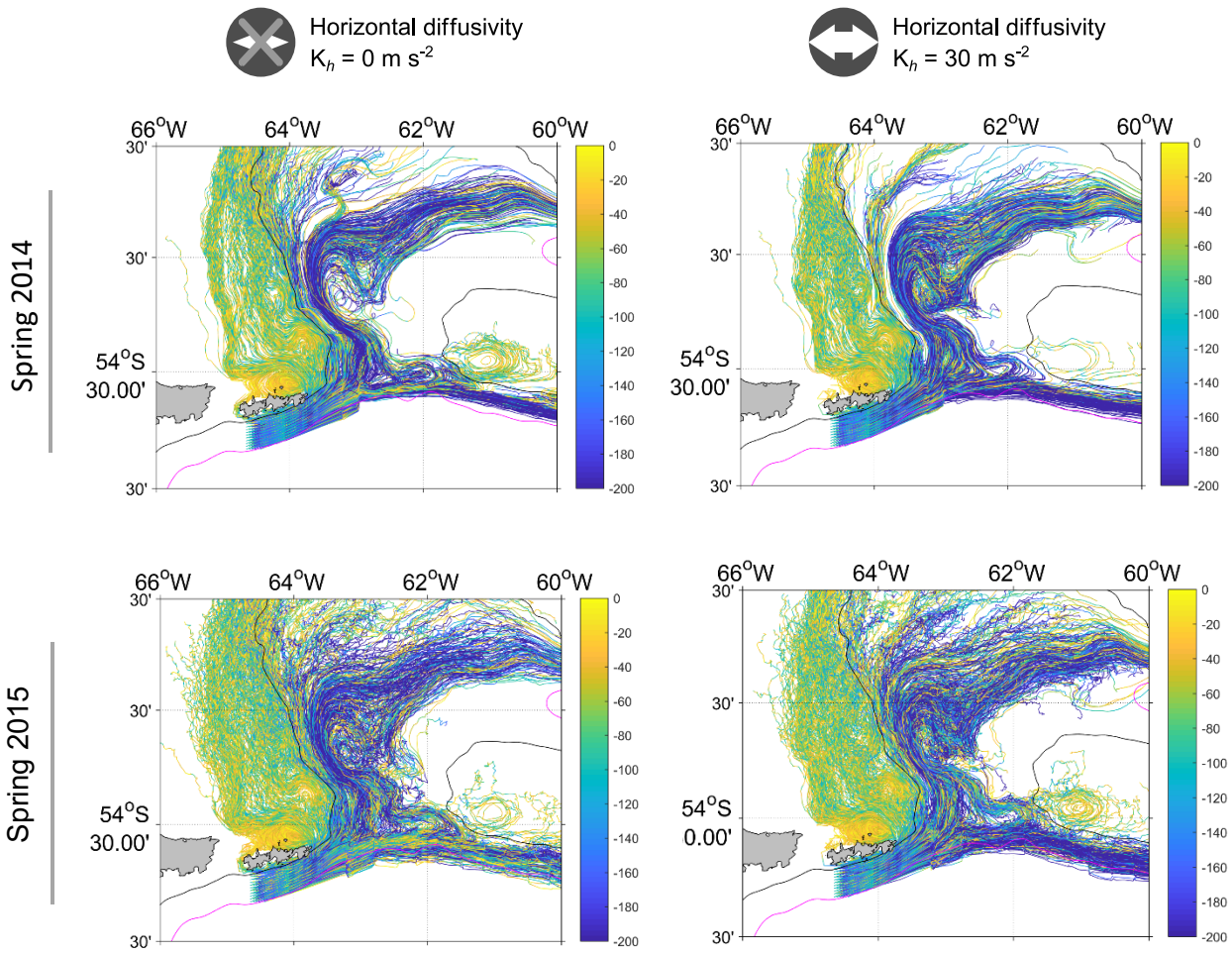

Fig. S3. Particle's trajectories from the tracking experiments using results from the hydrodynamical model forced with daily winds for two austral springs (2014 and 2015). Currents were averaged each five days and simulations were performed with and without horizontal diffusivity (K_h of 30 m s^{-2} and 0 m s^{-2} respectively) for Isla de los Estados (particularly complex hydrodynamic area within the study extent). Colours indicate the particle's depth.

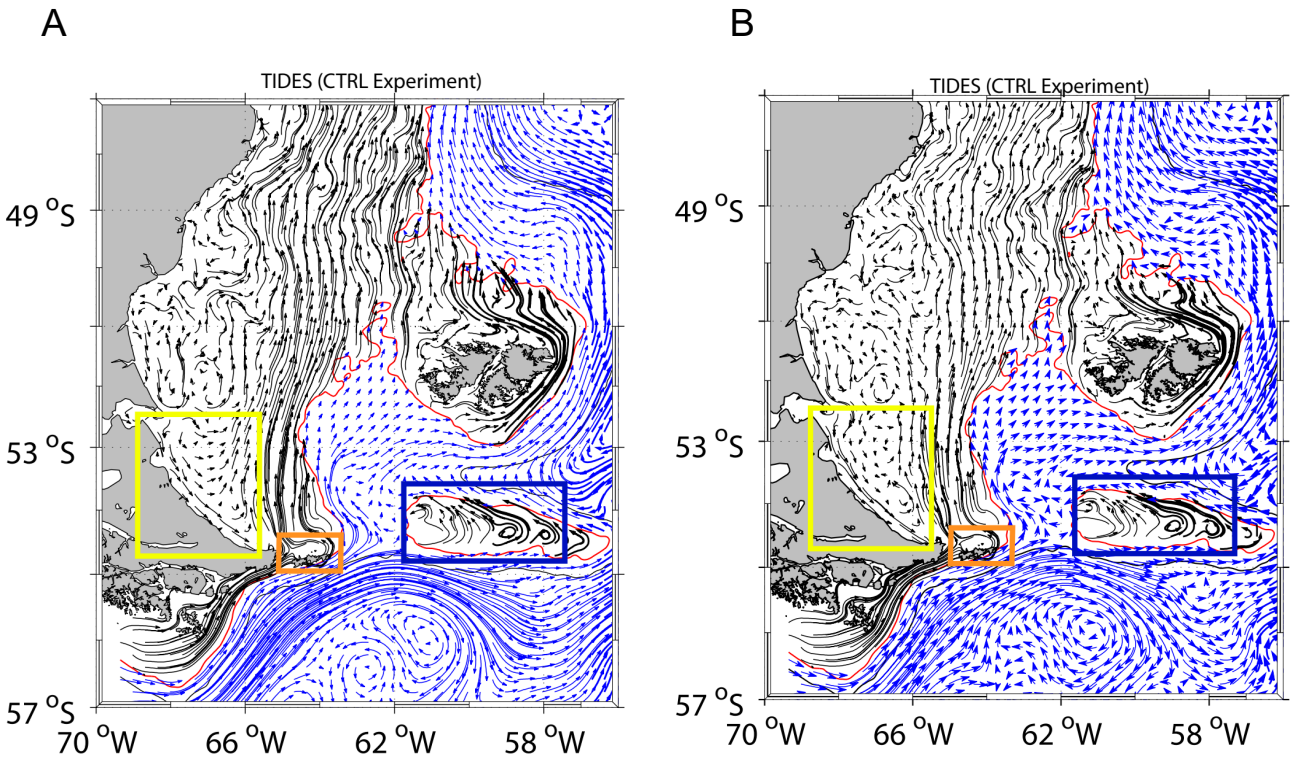

Fig. S4. Depth-averaged velocities depicting circulations patterns in the study are for the first 50 m (A) and for the total extent of the water column (B). Black and blue arrows indicate velocity vectors inside and outside the 200 m isobath (red line). Vortices are recognized within the Burdwood Bank (blue rectangle), north of Isla de los Estados (orange rectangle) and along the northern shelf of Tierra del Fuego (Yellow rectangle). The latter is beyond the extent of the samples analysed in this work.

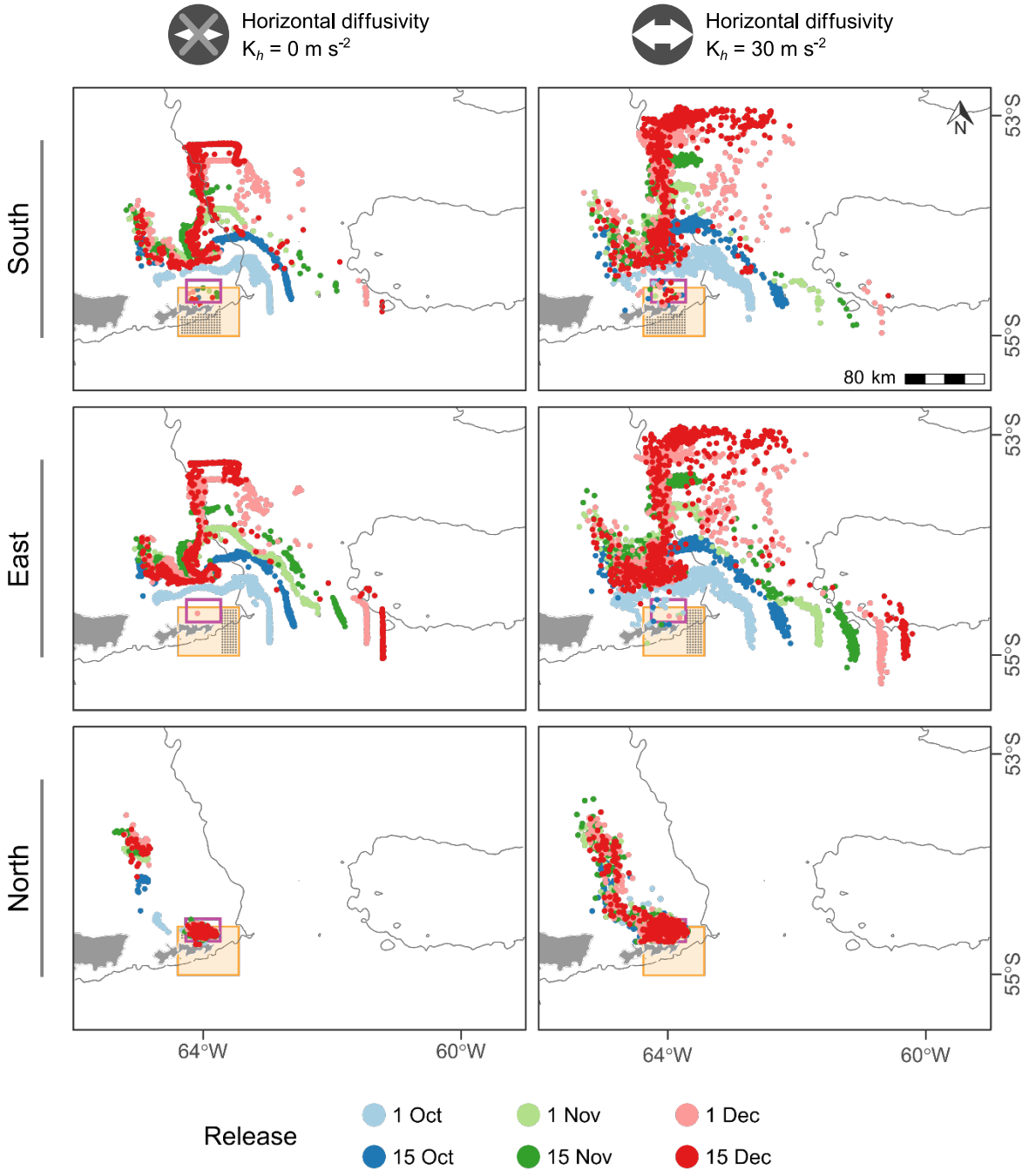

Fig. S5. Particle tracking simulations of particles released from Isla de los Estados according to the zone of release within the island (south, east or north). Results are shown for simulations without (K_h = 0 m s^{-2}) and with horizontal diffusivity (K_h = 30 m s^{-2}) and particles are differentiated according to the date of release.

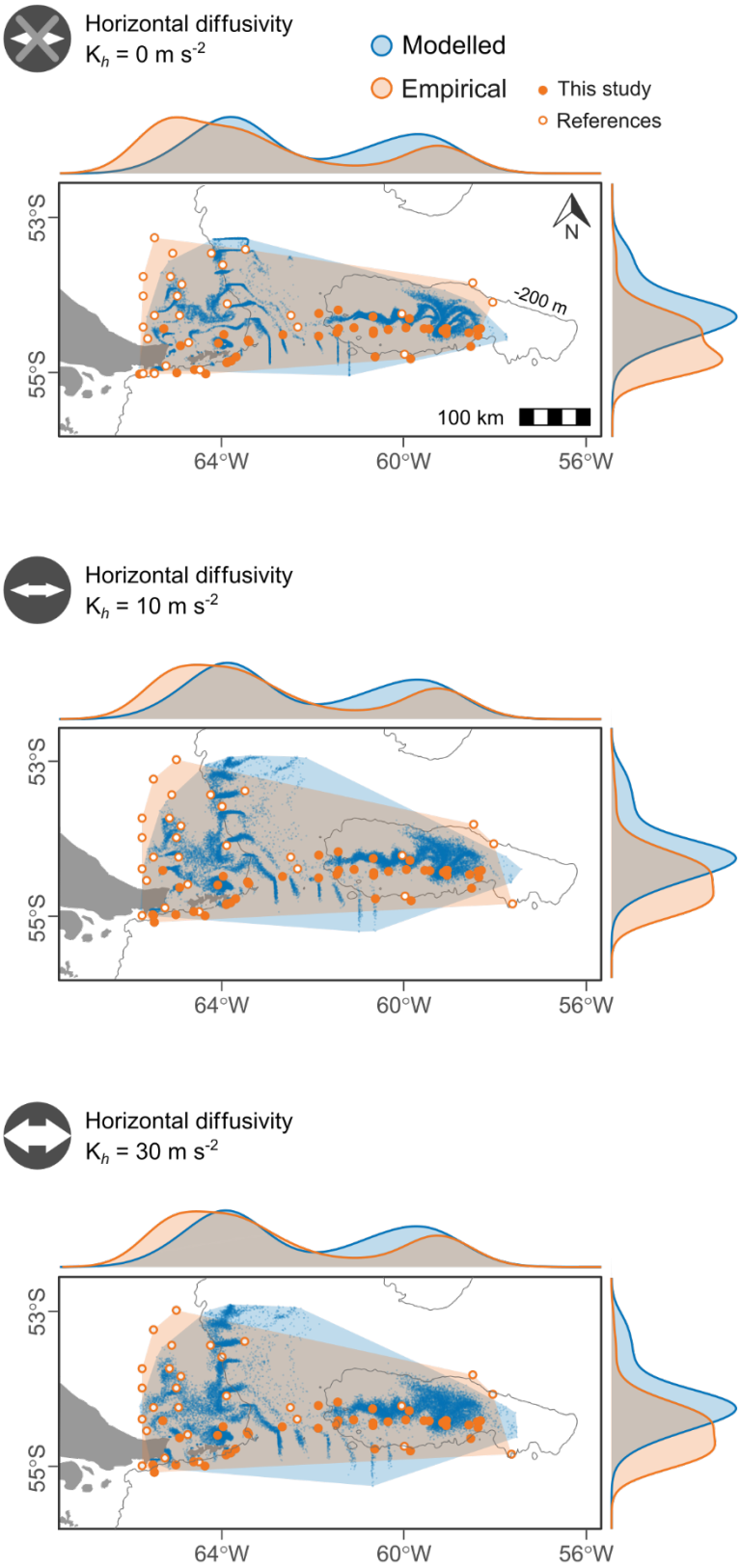

Fig. S6. Agreement between empirical and modelled data for simulations performed without (K_h = 0 m s^{-2}) and with horizontal diffusivity (K_h of 10 m s^{-2} and 30 m s^{-2}). Circles in the map represent particle's final positions (blue) and stations positive for Fuegian sprat early larvae sampled in austral spring and early summer (orange) during this (filled circles) and previous studies (empty circles). Density curves of longitudinal and latitudinal abundance distributions are shown at the top and right margin of the figure, respectively, for both types of data.

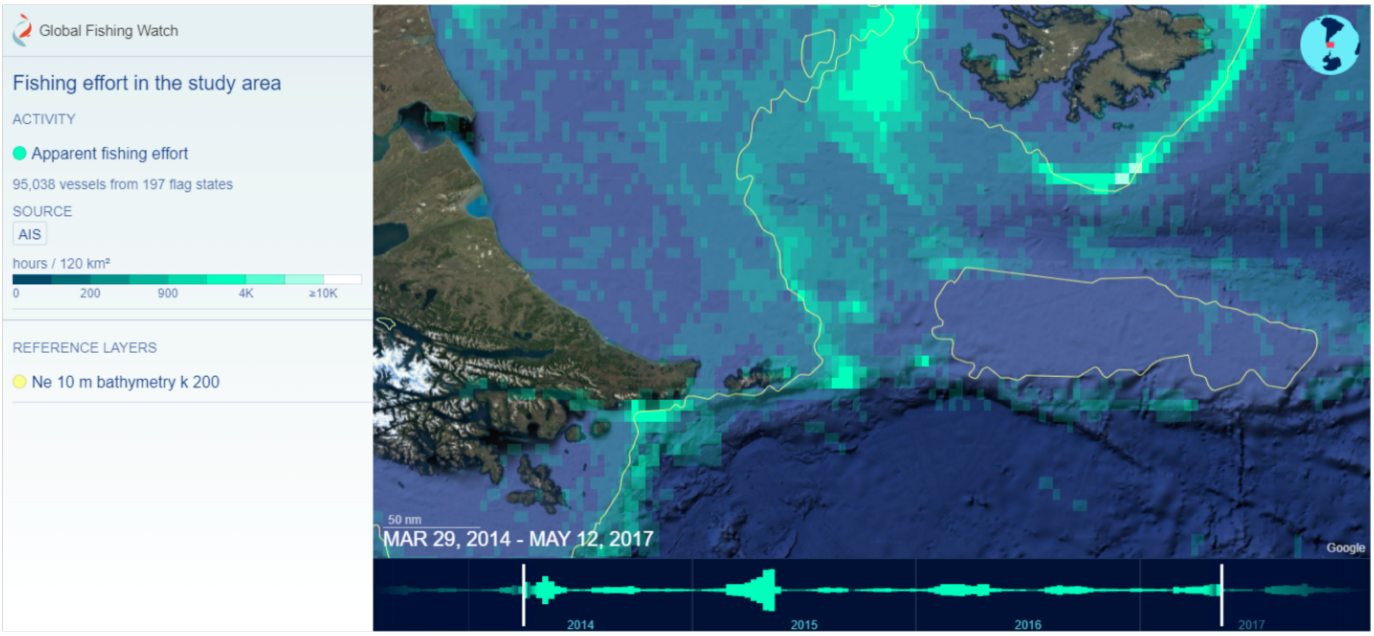

Fig. S7. Fishing effort in the study area during the time period when samples were collected (29/03/2014 - 12/05/2017). Data retrieved from Global Fishing Watch (https://globalfishingwatch.org/) and 200 m bathymetry downloaded from *Natural Earth* (1:10 m Physical Vectors; https://www.naturalearthdata.com/downloads/10m-physical-vectors/).